Bioresource Technology 320 (2021) 124411

Contents lists available at ScienceDirect

Bioresource Technology

journal homepage: www.elsevier.com/locate/biortech

Insights into the molecular transformation in the dissolved organic compounds of agro-waste-hydrochars by microbial-aging using electrospray ionization Fourier transform ion cyclotron resonance mass spectrometry

Qingnan Chu [a,b], Lihong Xue [a,c], Bingyu Wang [d], Detian Li [a], Huayong He [a], Yanfang Feng [a,c,f,*], Lanfang Han [e], Linzhang Yang [a], Baoshan Xing [f]

[a] Key Laboratory of Agro-Environment in Downstream of Yangtze Plain and Key Laboratory for Crop and Animal Integrated farming of Ministry of Agriculture and Rural Affairs, Ministry of Agriculture and Rural Affairs, Institute of Agricultural Resources and Environment, Jiangsu Academy of Agricultural Sciences, Nanjing 210014, China
[b] Graduate School of Agricultural and Life Sciences, The University of Tokyo, Yayoi, Bunkyo-ku, Tokyo 113-8657, Japan
[c] School of the Environment and Safety Engineering, Jiangsu University, Zhenjiang 212001, China
[d] Jiangsu Key Laboratory of Chemical Pollution Control and Resources Reuse, School of Environmental and Biological Engineering, Nanjing University of Science and Technology, Nanjing 210094, China
[e] Institute of Environmental and Ecological Engineering, Guangdong University of Technology, Guangzhou 510006, China
[f] Stockbridge School of Agriculture, University of Massachusetts, Amherst, MA 01003, USA

HIGHLIGHTS

- DOM of the pristine and microbial-aged hydrochars was comprehensively compared.
- Microbial-aging shifted highly oxygenated molecules into lower-order ones in DOM.
- Microbial-aging led to more biodegradable compounds and lower aromaticity of DOM.
- Microbial-aging promoted the degradation of phenols, phenolic acids, and PAH in DOM.
- Microbial-aging transforms the hydrochars-based DOM composition in a positive manner.

GRAPHICAL ABSTRACT

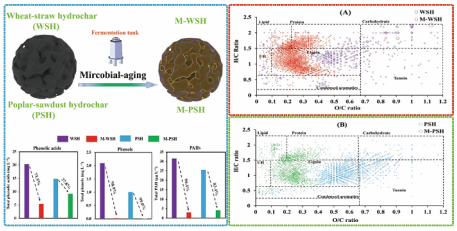

ARTICLE INFO

Keywords:
Anaerobic fermentation
ESI-FT-ICR-MS
Hydrothermal carbonization
Molecular composition
Polycyclic aromatic hydrocarbons

ABSTRACT

Hydrochars-based dissolved organic matters (DOM) are easily available to organisms and thus have important influence on the biota once applying hydrochars as environment amendment. Thus, positive modifications on molecular composition of DOM is indispensable before hydrochars application. In this study, the impacts of microbial-aging by anaerobic fermentation on DOM of agro-waste-hydrochars was systematically assessed. Results revealed that microbial-aging caused lower DOM release but higher DOM molecular diversity. Moreover, microbial-aging resulted in the production of more biodegradable compounds, including lipids and proteins, and

* Corresponding author at: Key Laboratory of Agro-Environment in Downstream of Yangtze Plain and Key Laboratory for Crop and Animal Integrated farming of Ministry of Agriculture and Rural Affairs, Ministry of Agriculture, Institute of Agricultural Resources and Environment, Jiangsu Academy of Agricultural Sciences, Nanjing, Jiangsu 210014, China.
E-mail address: yfeng@jaas.ac.cn (Y. Feng).

https://doi.org/10.1016/j.biortech.2020.124411
Received 1 October 2020; Received in revised form 9 November 2020; Accepted 10 November 2020
Available online 13 November 2020

reduced the aromaticity of DOM. The highly oxygenated molecules (O/C > 0.6) were shifted into lower-order ones in the hydrochars-based DOM, suggesting the transformation of hydrophilic compounds into hydrophobic ones. Additionally, microbial-aging promoted the degradation of phenols by 99.0–98.9%, phenolic acids 37.8–73.5%, and polycyclic aromatic hydrocarbons by 83.4–90.4% in hydrochar-based DOM. Overall, this study demonstrates that microbial-aging changes the molecular characteristics of hydrochars-based DOM in a positive manner.

1. Introduction

Biochar is a carbon-rich material converted from biomass pyrolyzed in a closed container at 300–600 °C with high pressure under oxygen-limited conditions (Zhu et al., 2018; Haeldermans et al., 2020) or hydrothermal carbonization (HTC) in the presence of feedwater (called hydrochar hereinafter) at 180–260 °C (Yu et al., 2019a; Ponnusamy et al., 2020). Producing biochars can transform the wastes into valuable resources, as reflected in multiple studies that applied biochars to reduce nutrient leaching from the soil (Chu et al., 2020b), improve soil fertility (Yu et al., 2019a), and inhibit greenhouse gas emissions (Awasthi et al., 2016; Chu et al., 2020a). Compared with traditional pyrolysis, HTC is generally more energy-efficient because of its relatively lower temperature and autogenous pressure (Chu et al., 2020b; Sztancs et al., 2020). Moreover, hydrochars showed lower thermal stability (Wang et al., 2020b) and thus own dozens or hundreds of times higher DOM than biochars made by pyrolysis (Song et al., 2020). For instance, DOM extracted from the pig manure-derived hydrochar and biochar ranged from 3.3–12.0% and 0.4–0.5%, respectively (Song et al., 2020). Despite less than 10% content of hydrochars, DOM are easily available to microorganisms, microalgae, or plants as carbon source and thus have important influence on the biota once applying hydrochars into the environment (Sun et al., 2020; Wang et al., 2018; Yu et al., 2019). Therefore, a comprehensive analysis needs to be done to profile the hydrochar-based DOM.

Because hydrochar-based DOM is highly complex and a polydisperse mixture of organic compounds, the molecular composition has been seldom investigated. Most of the literature focuses on the use of ultraviolet–visible spectrometry and gas chromatography-mass spectrometry (GC–MS) to analyze the characteristics of hydrochars-based DOM that has diverse compositions (Rombolà et al., 2015; Smith et al., 2016; Oleszczuk and Kołtowski, 2018). Unfortunately, these characterization methods could only analyze the targeted and limited compounds but fail to profile the composition of hydrochars-based DOM at molecular level. With rapid advancement of mass-spectrometric techniques, electrospray ionization (ESI) combined with the Fourier transform ion cyclotron resonance mass spectrometry (FT-ICR-MS) has proven to be a remarkable tool for the analysis of organic matters composition at the molecular level, such as DOM of compost (Yu et al., 2019b) and sewage sludge (Yuan et al., 2019). Owing to its high resolution (300,000–40,0000) and mass accuracy (<0.5 ppm), this cutting-edge technique can simultaneously distinguish thousands of different compounds in one sample and calculate the elemental formulas for every individual mass peak (Koch and Dittmar, 2006). However, only few studies have investigated the hydrochars-based DOM using ESI-FT-ICR-MS (Hao et al., 2018; Sun et al., 2020).

Furthermore, the degradation of polymers (cellulose, hemicellulose, and lignin) and recondensation of small molecules during HTC yield some condensed aromatics and phenols, which are potentially toxic and mutagenic (Wiedner et al., 2013; Zhou, 2014; Hao et al., 2018). In recent studies, DOM from hydrochars have been demonstrated to dramatically inhibit microalgal growth when used as a culture medium (Smith et al., 2016; Hao et al., 2018). Therefore, failure to effectively pretreat the hydrochars before application could cause environmental pollution with the side-effect of hydrochars-based DOM. Microbial-aging is a cost-effective way to transform the molecular compounds in a positive manner and promote the depolymerization of noxious components in DOM through the role of biodegradation (Yu et al., 2019a; Oleszczuk and Kołtowski, 2018; Hua et al., 2020; Quan et al., 2020). Previous studies stated that toxic compounds are removable by microbial treatment through increasing the hydrophobicity of biochars to reduce the binding strength between these compounds and the biochar surface functional group as well as intrinsic minerals (Rombolà et al., 2015; Oleszczuk and Kołtowski, 2018; Quan et al., 2020). Moreover, microbial-aging promoted the humification of DOM to modify the polycyclic aromatic hydrocarbons (PAHs) with aromatic fulvic- and humic-structures to improve soil fertility and plant growth (Yang et al., 2019; dos Santos et al., 2020; Quan et al., 2020). With lower thermal stability and more abundant DOM (Garlapalli et al., 2016), more hydrogenic C is supposed to be degraded by microbial-aging. However, a dearth of information has been known regarding the microbial-aging effects on DOM composition of hydrochars.

This study aims to comprehensively investigate the molecular composition of DOM released from the pristine and microbial-aged hydrochars to provide the theoretical basis for developing more environment-friendly hydrochars. Anaerobic fermentation was applied to microbially age the agro-waste-derived hydrochars. The changes in the molecular composition characteristics of hydrochars-based DOM were comprehensively analyzed using ESI-FT-ICR-MS. The changes of potentially noxious compounds were investigated as well, including PAHs, phenolic acids, and phenols.

2. Materials and methods

2.1. Hydrochar preparation and microbial-aging modification

Wheat straw and poplar sawdust, which are common agricultural wastes, were used as the biomass feedstock for hydrochar production. HTC was conducted in a hydrothermal reactor (autogenerated pressure during HTC) using a solid to liquid ratio of 1:10. The reactor was sealed and heated at 260 °C for 1 h and then allowed to naturally cool down to room temperature overnight. The inoculum for microbial-aging was prepared through anaerobic fermentation as described in a previous study (Yu et al., 2019a). Briefly, the aging inoculum was prepared by mixing 11 kg straw or sawdust with 100 L biogas slurry in a 150 L anaerobic fermentation bucket. Then the inoculum was mixed with 3.78 kg of sawdust- or straw-derived hydrochars. The pH in the fermenter was kept in the range of 6–8, and after 60 d of aging the resulting solid products were recovered from the fermenter, washed, dried, ground, and sieved using a 0.3 mm mesh. The pristine wheat straw- and poplar sawdust-hydrochars were labeled as WSH and PSH, while the microbial-aged ones were labeled as M-WSH and M-PSH, respectively.

The total carbon (C), nitrogen (N), hydrogen (H), and oxygen (O) concentration of hydrochars were determined using an Elemental Analyzer (EL III; Elementar Analysensysteme GmbH, Germany). Thermogravimetric analyses were conducted to evaluate the stability of hydrochars using the thermogravimetric analyzer-SDT Q600 (USA). The pH of the hydrochars was obtained by analyzing the solid/deionized water ratio of 1:2.5 (w/v) using a pH meter. The cation exchange capacity (CEC) of hydrochars was measured according to a previous study (Chu et al., 2017). The specific surface area (SSA) and porosity were measured using a NOVA 1200 analyzer (Anton Paar QuantaTec Inc., Graz, Austria), and were calculated by the Brunauer-Emmett-Teller method (Chu et al., 2020c).

2.2. DOM extract and characterization

DOM was extracted from the hydrochars as described in a previous study (Hua et al., 2020). A portion of the extracted DOM was digested using perchloric acid and the aqueous extract was determined by a TOC analyzer (Multi N/C 2100, Germany). Other DOM samples were frozen at −80 °C for molecular composition analysis. The concentration of total phenolic acids, including *p*-coumaric, vanillic, *p*-hydroxybenzoic, syringic, caffeic, ferulic, and sinapic acid, were analyzed as described in a previous study (Blum et al., 1991). The phenol compound was analyzed using GC–MS (7890/5975C, Agilent, USA). The PAHs were analyzed in the DOM by GC–MS according to the method in a previous study (Liu et al., 2018).

ESI-FT-ICR-MS analysis was performed on a Bruker SolariX FT-ICR-MS equipped with a 15.0 T super-conducting magnet and dual-mode electrospray ionization/matrix-assisted laser desorption ionization ion source, as described in the previous study (Riedel et al., 2012). Each sample was analyzed in triplicate and averaged. Briefly, ultrahigh resolution mass spectra were acquired using a Bruker Solari X FT-ICR-MS equipped with a 15.0 T super-conducting magnet and a dual-mode ESI/MALDI ion source. Samples for ESI-FT-ICR-MS analysis were continuously infused into the ESI/MALDI ion source. DOM samples for ESI-FT-ICR-MS analysis were continuously infused into the ESI unit by syringe infusion at a flow rate of 120 μL h^{-1}. The ESI needle voltage was set to −3.8 kV. All samples were analyzed in negative ionization mode with broadband detection. Ions were accumulated in a hexapol ion trap for 0.06 s before being introduced into the ICR cell. The 4 M word size was selected for the time domain signal acquisition. The mass limit was set between 160 and 1000 Da. The quality assurance/quality control (Q_A/Q_C) was conducted to filter the dataset: (1) the spectra were externally calibrated with 10 mM of sodium format solution in 50% isopropyl alcohol using a linear calibration, and then internally recalibrated using an in-house reference mass list. After internal calibration, the mass error was less than 500 ppb over the entire mass range for the reference mass list. (2) Peaks observed in deionized water or solvent blanks were removed. (3) Every sample was analyzed thrice, and only peak which could be detected by triplicate analysis and had the relative abundance over five times the standard deviation of the baseline noise was retained. The averaged molecular information was then exported to an excel spreadsheet and used for further analysis.

2.3. Calculation formulas of parameters

All possible formulas were calculated with Formula Calculated software based on the requirement that the mass error between the measured mass and the calculated mass for a given chemical formula that is less than 0.5 ppm, and the signal-to-noise ratio of mass peaks exceeds 5. The elemental ratios of H/C < 2.5 and O/C < 1.2 were used as restrictions for formula calculation. H/C ratio and O/C ratio was calculated to classify the biomolecular compounds into seven categories as lipid, proteins, carbohydrate, unsaturated hydrocarbon, lignin, tannin, and condensed aromatic. Double bond equivalence (DBE) for analyzing the number of double bonds and rings in a molecule was to evaluate the degree of unsaturation and aromaticity (Stenson et al., 2003); nominal oxygen state of carbon (NOSC) to evaluate the oxidation degree and molecular polarity/hydrophobicity of compounds; an aromaticity index (AI) to estimate the fraction of aromatic structures (Riedel et al., 2012).

From the molecular formula ($C_cH_hO_o$) assignments, the double bond equivalent (DBE) and modified aromaticity index (AI) can be expressed as:

$$DBE = 1 + (2c - h)/2 \quad (1)$$

$$AI = (1 + c - o/2 - h/2)/(c - o/2) \quad (2)$$

$$NOSC = 4 - -[(4c + h - -2o)/c] \quad (3)$$

where c, h, and o refer to the stoichiometric numbers of carbon, hydrogen, and oxygen atoms per formula, respectively.

The magnitude-averaged C, H, O, O/C, H/C, molecular weight, AI, and DBE values for each sample can be determined as follows:

$$Mw = (\text{å}_i I_i{*}M_i)/\text{å}_i I_i \quad (4)$$

where M represents parameters C, H, O, O/C, H/C, molecular weight, AI, and DBE, respectively, *w* signifies a magnitude-weighted calculation, and Ii and Mi are the relative abundance and M value of peak, respectively. The relative abundance is calculated as the abundance of the individual peak divided by the standard peak in a given spectrum.

3. Results and discussions

3.1. Changes of basic characteristics in microbial-aged hydrochars

Applying anaerobic fermentation to age the hydrochars microbial-aging increased C and decreased H, O, and N content of hydrochars, both in M-WSH and M-PSH, which concurs with previous studies (Yu et al., 2019a; Hua et al., 2020). The loss of H, O, and N was likely attributed to the anaerobic gasification, such as methane, carbon dioxide, and ammonia (Huang et al., 2015; Deaver et al., 2020). These changes included a decline in the atomic ratios of O/C and H/C, suggesting a promoted dehydration (Fig. 1A), decreased polarity, and an increased affinity for hydrophobic organic contaminants during the microbial-aging process (Oleszczuk and Kołtowski, 2018; Rombolà et al., 2015). Additionally, microbial-aging increased the pH of WSH and PSH from 3.71 and 4.77 to 6.60 and 7.04, supported by previous reports on microbial-aged sawdust hydrochars (Yu et al., 2019a; Hua et al., 2020). Also, the CEC of hydrochars was increased from 9.22–11.97 to 15.93–24.53 cmol kg^{-1} after microbial-aging, which is beneficial for providing more adsorption sites for nutrients retention and contaminant immobilization when applied as soil amendment (Hua et al., 2020; Sun et al., 2020; Sha et al., 2020).

Furthermore, Fig. 1B depicts that microbial activity markedly increased the SSA and porous volume in both M-WSH and M-PSH, consistent with previous studies on microbial-aged lignocellulosic biochar or hydrochars (Yu et al., 2019a; Quan et al., 2020; Hua et al., 2020). These results suggest that microbial-aging substantially changed the surface morphology and improved the adsorption capacity of hydrochars. The thermogravimetric analyses showed that microbial-aged hydrochars had lower recalcitrance, as revealed by a lower retention thermogravimetry and higher weight loss (Fig. 1C) (Harvey et al., 2012). Thermogravimetry (TG)-derivative thermogravimetry (DTG) curves were divided into four mass loss regions at four specific temperature intervals following previous studies (Cimò et al., 2014). In all four regions, microbial-aged hydrochars showed more mass loss than pristine hydrochars. Relatively higher mass loss of four hydrochars was observed in Region II (210 °C–420 °C) and III (420 °C–570 °C); M-WSH and M-PSH lost markedly greater mass than WSH and PSH. The mass loss that occurred in microbial-hydrochars was mainly assigned to the thermo-oxidative degradation of labile aliphatic acids, alkyl systems, and carbohydrates (Region II; Lopez-Capel et al., 2005) and the pyrolysis of more recalcitrant aromatic moieties (Quan et al., 2020; Cimò et al., 2014). Also, the lower recalcitrance in microbial-aged hydrochars indicated that they might have lower aromaticity (Harvey et al., 2012). Overall, microbial-aging strongly changed the properties of hydrochars and potentially affected the hydrochar-based DOM release into the environment.

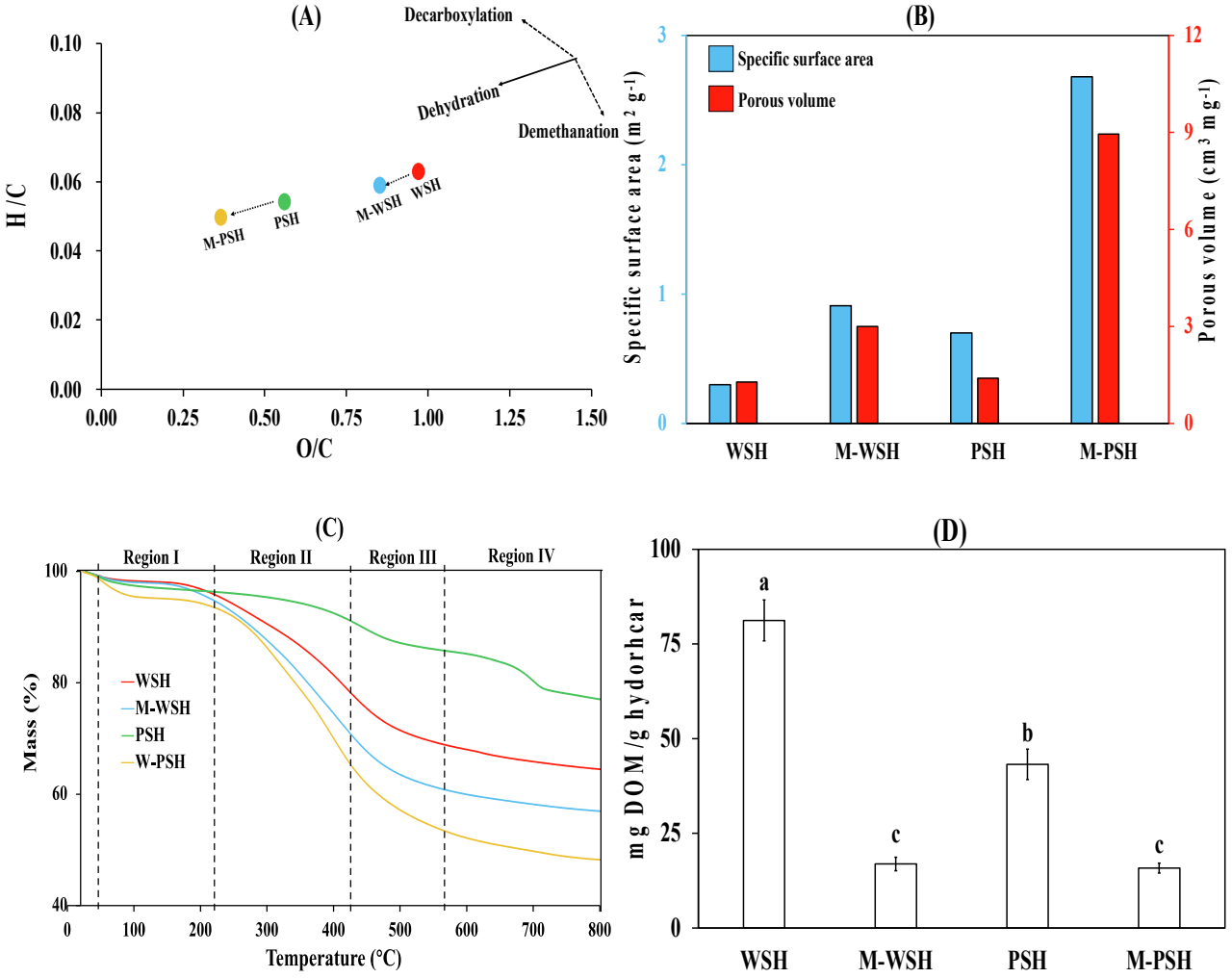

Fig. 1. Effects of microbial-aging on (A) H/C and O/C ratios for hydrochar samples based on the analysis by Elemental Analyzer; (B) the special specific area and porous volume; (C) thermogram plots of hydrochars; (D) the DOM content of four different hydrochars. M-PSH" microbial-aged poplar sawdust-derived hydrochars; M-WSH: microbial-aged wheat straw-derived hydrochars; PSH: poplar sawdust-derived hydrochars; WSH: wheat straw-derived hydrochars.

3.2. Microbial-aging increased the diversity and biodegradability of hydrochars-based DOM

The DOM concentrations released from the microbial-aged hydrochars—M-WSH and M-PSH both decreased by 4.8- and 2.7-fold, compared to WSH and PSH, respectively (Fig. 1D). This result concurred with previous studies on the decreased hydrochar-based DOM after microbial-aging (Yu et al., 2019a; Hua et al., 2020), but disagrees with those concerning the DOM of biochars produced by pyrolysis (Smith et al., 2016; Oleszczuk and Kołtowski, 2018; Quan et al., 2020). This difference might be attributed to the higher thermal stability and recalcitrance, as well as the lower initial DOM content in the pyrogenic biochars (Garlapalli et al., 2016; Quan et al., 2020). The molecular weight distribution of DOM is shown in the ESI-FT-ICR-MS broadband spectra. Broadband spectra of hydrochars-based DOM all spanned a similar molecular weight range (150–650 ~ m/z). Thousands of molecular formulas of DOM were identified by assigning the molecular formula ($C_aH_bO_c$) to each peak (Riedel et al., 2012). Microbial-aging resulted in increased molecular diversity of DOM, as revealed in the number of assigned peaks, which increased from 1456 in WSH to 2197 in M-WSH, and from 2091 in PSH to 2653 in M-PSH. The increased number of organic compounds indicated the progression of depolymerization reactions during microbial-aging (Hao et al., 2018; Wang et al., 2020a). Overall, microbial-aging resulted in dramatically lower amount of DOM release from hydrochars but higher diversity of DOM molecular composition.

Given that high resolution mass spectral analyses are capable of determining the molecular compositions of DOM samples, visualization of properties of hydrochars-based DOM was completed by calculations and statistics about ESI-FT-ICR-MS data and the combination of O/C and H/C and van Krevelen (VK) diagrams (Fig. 2A and 2B). In the VK diagrams, each point represented one molecule. According to previous studies, VK-diagrams plot assigned molecular formulas into seven clusters based on their molar H/C (y-axis) and O/C (x-axis) ratios (Koch and Dittmar, 2006; Smith et al., 2016; Sun et al., 2020). The results revealed a notable watershed between the DOM of pristine and microbial-aged hydrochars in the V/K diagram (Fig. 2A and 2B), which displayed that microbial-aging transformed most of the high O/C compounds (>0.6) into those with low O/C (<0.4), irrespective of the feedstock of hydrochars, which might be attributed to the role of microbial deoxygenation during anaerobic fermentation. More compounds with lower O/C atomic ratios were produced in the DOM of microbial-aged hydrochars, consistent with the changes in hydrochar materials. Also, lignin was the dominant compound in DOM in all four hydrochars, occupying 40.1%-61.2% of the compound's abundance (Fig. 2C). The mass generation of lignin was possibly associated with the feedstock of lignocellulosic materials and similar results have been found in bamboo-derived hydrochars (Hao et al., 2018). Although the abundance of lignin was

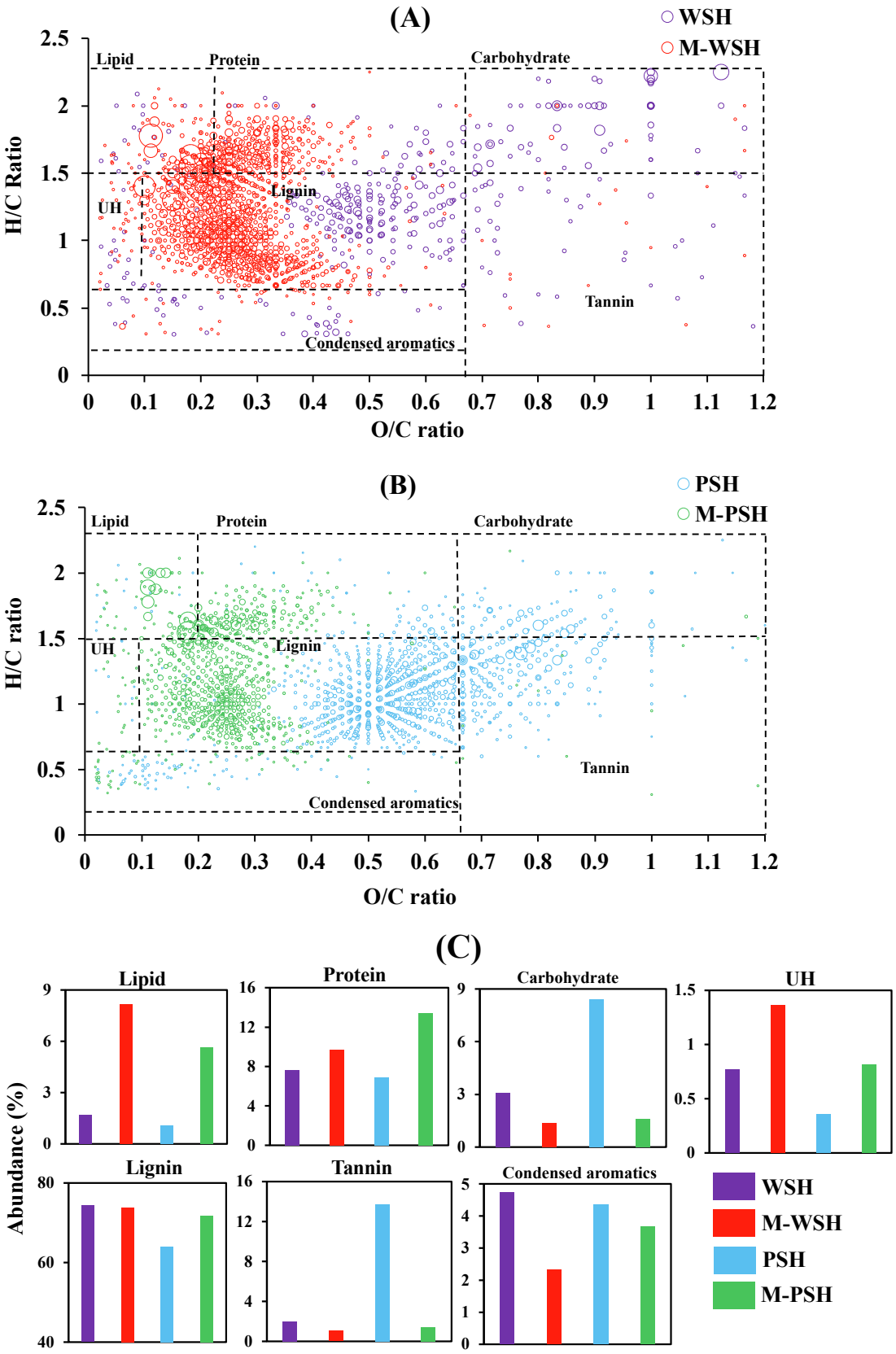

Fig. 2. Van Krevelen (VK) plots for CHO molecular formulas assigned to the ESI FT-ICR MS spectral peaks in (A) WSH and M-WSH; (B) PSH and W-PSH, and the abundances of seven types of biomolecular compounds in the DOM of different hydrochars are shown in (C). The size of sphere in (A) and (B) represents the relative e abundance of one type of molecular formula. UH: unsaturated hydrocarbon.

comparable among the four hydrochars, lignin with higher O/C ratio (0.35–0.67) in WSH and PSH-based DOM was transformed into lower O/C ratio (0.10–0.35) in M-WSH and M-PSH-based DOM. Similarly, studies also proved a remarkable increase in the proportion of lignin-like components in DOM derived from the native soil amended with WSH (Sun et al., 2020).

Microbial-aging led to markedly lower abundance of carbohydrate, tannin and condensed aromatics, and higher abundance of lipid, protein, unsaturated hydrocarbon in the M-WSH- and M-PSH-based DOM (Fig. 2C). Among the seven classes of compounds, lipids, proteins, and carbohydrates ($2.2 \geq H/C \geq 1.5$) owns the relatively higher bioavailability (Yu et al., 2019b). Although microbial-aging resulted in the decrease of carbohydrate compounds from 5.7% and 8.8% in WSH and PSH to 1.6% and 1.9% in the DOM of M-WSH and M-PSH, the total amount of lipids, proteins, and carbohydrates was increased from 16.8% and 16.5% in the WSH- and PSH-based DOM to 22.1% and 21.2% in M-WSH and M-PSH-based DOM. The release of these bioavailable aliphatic compounds is more biodegradable in the environment. Upon applying the microbial-aged hydrochars for soil amendment, the more biodegradable DOM is beneficial for providing carbon source for microorganisms to promote the microbial activity and increase community diversity (Sun et al., 2020), which further helps nutrients mineralization and increase nutrients availability for plants (Hall et al., 2020). In addition, microbial-aging reduced the abundance of tannins by 47.2% in M-PSH and 89.6% in M-WSH, and the abundance of condensed aromatics by 25.1% in M-PSH and 26.4% in M-WSH. The decrease of these recalcitrant compounds might partly contribute to the increase of the biodegradable lipids and proteins. Meanwhile, the analysis of aromatic index (AI) further demonstrated that microbial-aging led to markedly higher aromatics and lower condensed aromatic compounds (7.1% in WSH and 2.9% in M-WSH, 8.8% in PSH and 2.1% in M-PSH) in DOM, suggesting the decrease of aromaticity. Microbial activity likely

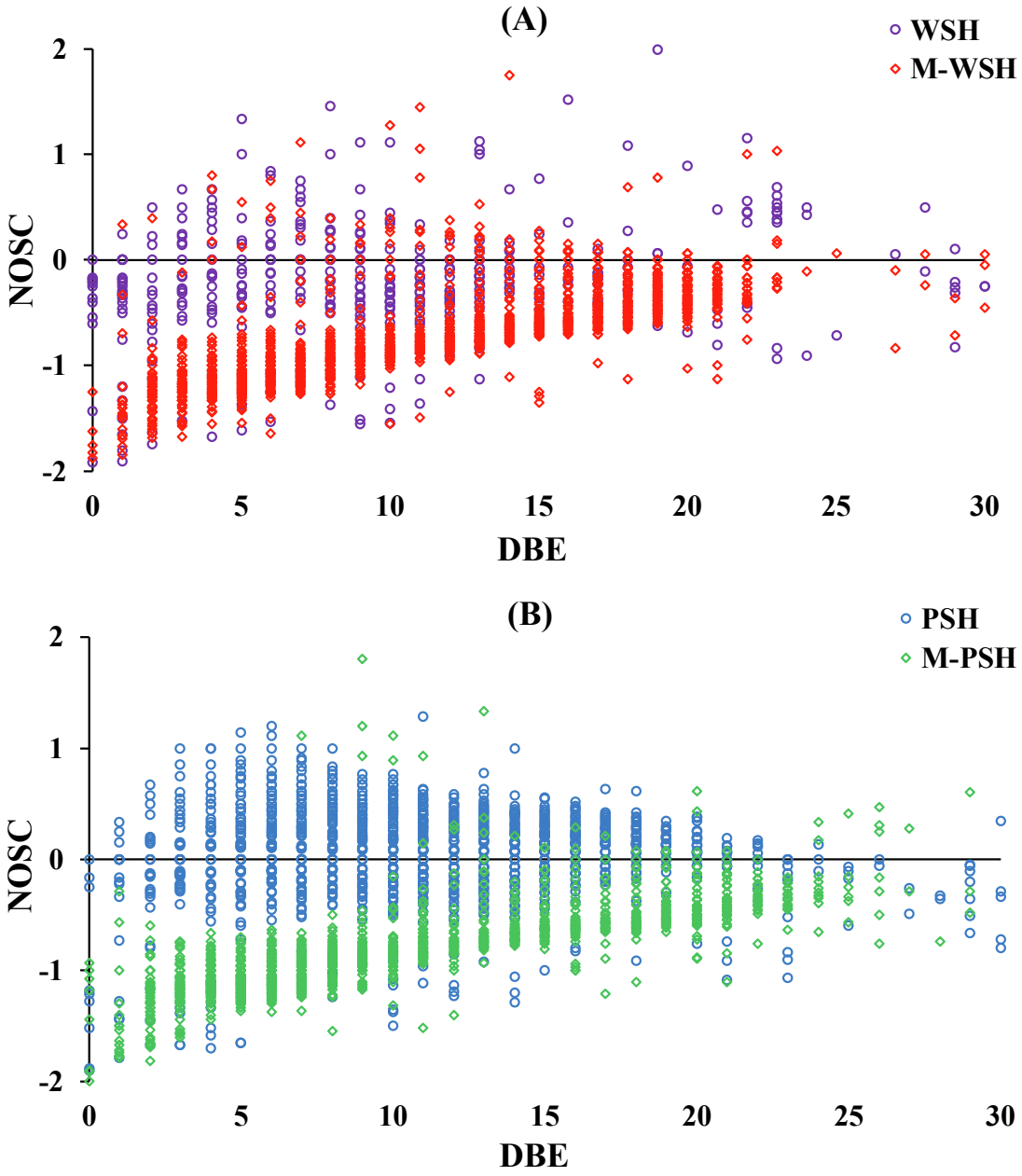

Fig. 3. Double-bond equivalence (DBE) versus nominal oxidation state of carbon (NOSC) of the four hydrochar-based DOM, based on the data from negative-ion ESI-FT-ICR-MS. WSH and M-WSH (A), and of PSH and M-PSH (B).

promoted the cracking of condensed aromatic compounds to produce more monocyclic aromatics in hydrochars-based DOM (Oleszczuk and Kołtowski, 2018; Quan et al., 2020). Overall, microbial-aged hydrochars-based DOM displayed more biodegradable molecular compositions and lower aromaticity.

3.3. Microbial-aging reduced the oxidation degree and increased the hydrophobicity of hydrochars-based DOM

Organic compounds with O/C ratios greater than 0.6 are usually hydrophilic and have been shown to be highly mobile in soil (Stenson et al., 2002). The degree of unsaturation and solubility of DOM can be analyzed by plotting DBE against NOSC (Fig. 3). The NOSC of almost all the compounds from M-WSH- and M-PSH-based DOM was negative; however, the NOSC of almost half of the compounds from WSH- and PSH-based DOM was positive. Negative NOSC values dominate in DOM of microbial-aged hydrochars, which was indicative of a lower polarity and higher hydrophobicity (Stenson, 2008; Riedel et al., 2012). These results implied that microbial-aging drove the shift of hydrophilic molecules to the hydrophobic ones in DOM. The reduction of oxidation degree and polarity might be associated with the decrease of carbohydrates abundance and increase of lipids, as shown in Fig. 2C. Moreover, the increase in hydrophobicity in hydrochars-based DOM was beneficial for the decrease in the source of hydrophilic noxious compounds, such as phenols, and retarding the compounds released from hydrochars into the environment. These results suggest that microbial-aging could help retard the compounds release from hydrochars upon application to the soil.

Fig. 4 depicts the detailed variations of each class of C_x species (organic compounds with x carbon atoms) and DBE among the four types of hydrochars-based DOM. A similar relationship between C number and DBE was observed for hydrochars before and after microbial-aging (Fig. 4A, 4B, 4C, and 4D), although microbial-aging increased the diversity of each class of compound. The most abundant compounds of WSH- and PSH-based DOM were both located at DBE value of 1; however, those of M-WSH- and M-PSH-based DOM were located at DBE value of 6 and 8, respectively. This shift to higher DBE by microbial-aging suggested that the most abundant compounds in DOM became more unsaturated and formed more long-chain fatty acids or condensed aromatics, which was likely driven by the deoxygenation and recondensation reactions that occurred in the process of anaerobic microbial-aging (Ge et al., 2015; Rodríguez-Méndez et al., 2017).

The possibilities of changes into long-chain fatty acids or condensed aromatics in DOM could be elucidated with the exact DBE value and C number (Fig. 5). The most abundant molecule in WSH- and PSH-based DOM was $C_6H_{11}O_6$, which only had one double-bond (DBE = 1). With DBE equal to 1, more long-chain organic acids ($C_{18}H_{35}O_2$, octadecanoic acid, in M-WSH and $C_{16}H_{31}O_2$, hexadecanoic acid, in M-PSH) were formed in the DOM of microbial-aged hydrochars (Fig. 5A and 5C). The most abundant molecule in M-WSH-based DOM was $C_{13}H_{15}O_4$ with six double-bond (DBE = 6) (Fig. 5B) and in M-PSH was $C_{15}H_{15}O_5$ with eight double-bond (DBE = 8) (Fig. 5D), suggesting that long-chain fatty acids

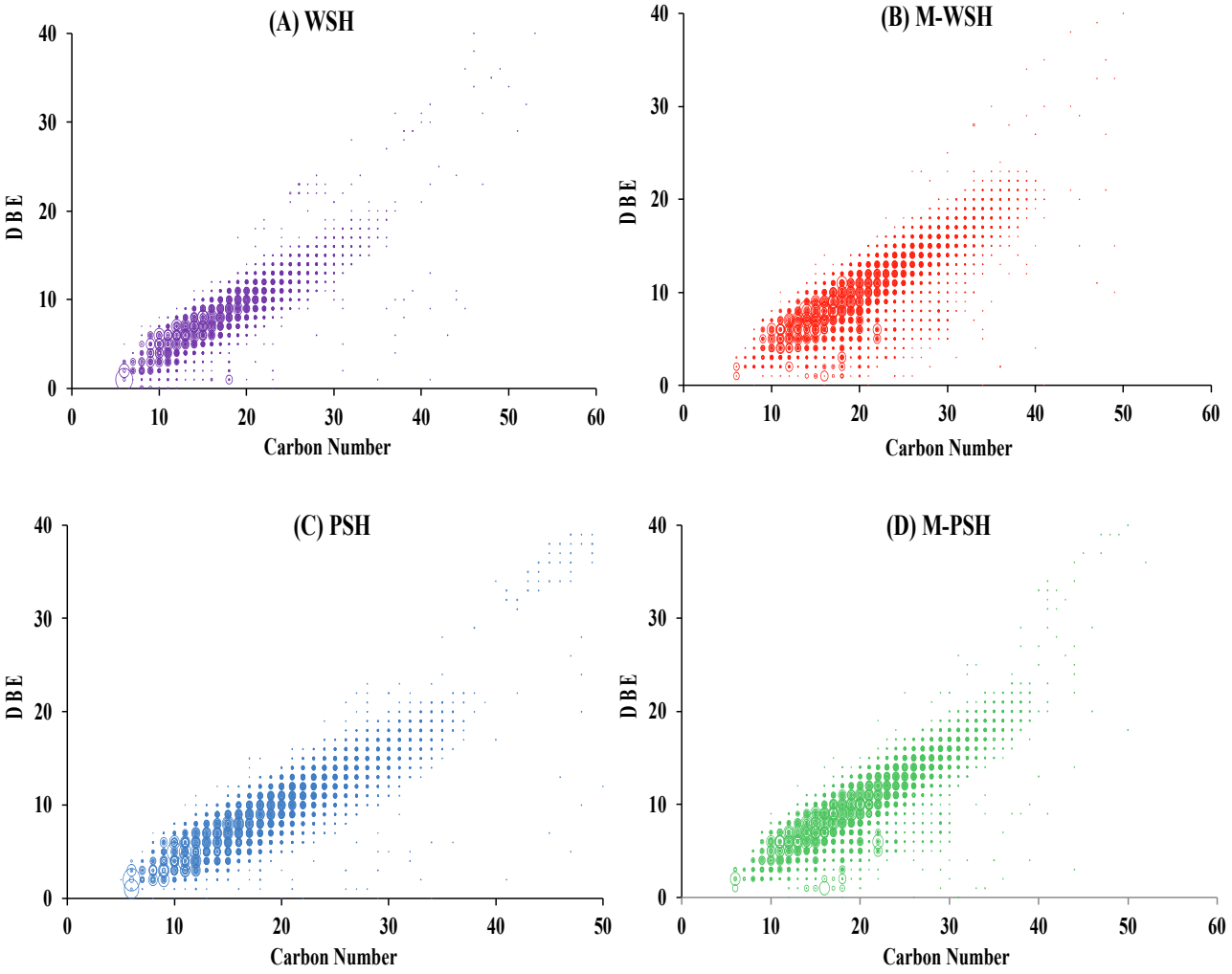

Fig. 4. Carbon number versus DBE (double-bond equivalent) distribution in the DOM of WSH (A), M-WSH (B), PSH (C), and M-PSH (D) detected by ESI FT-ICR MS.

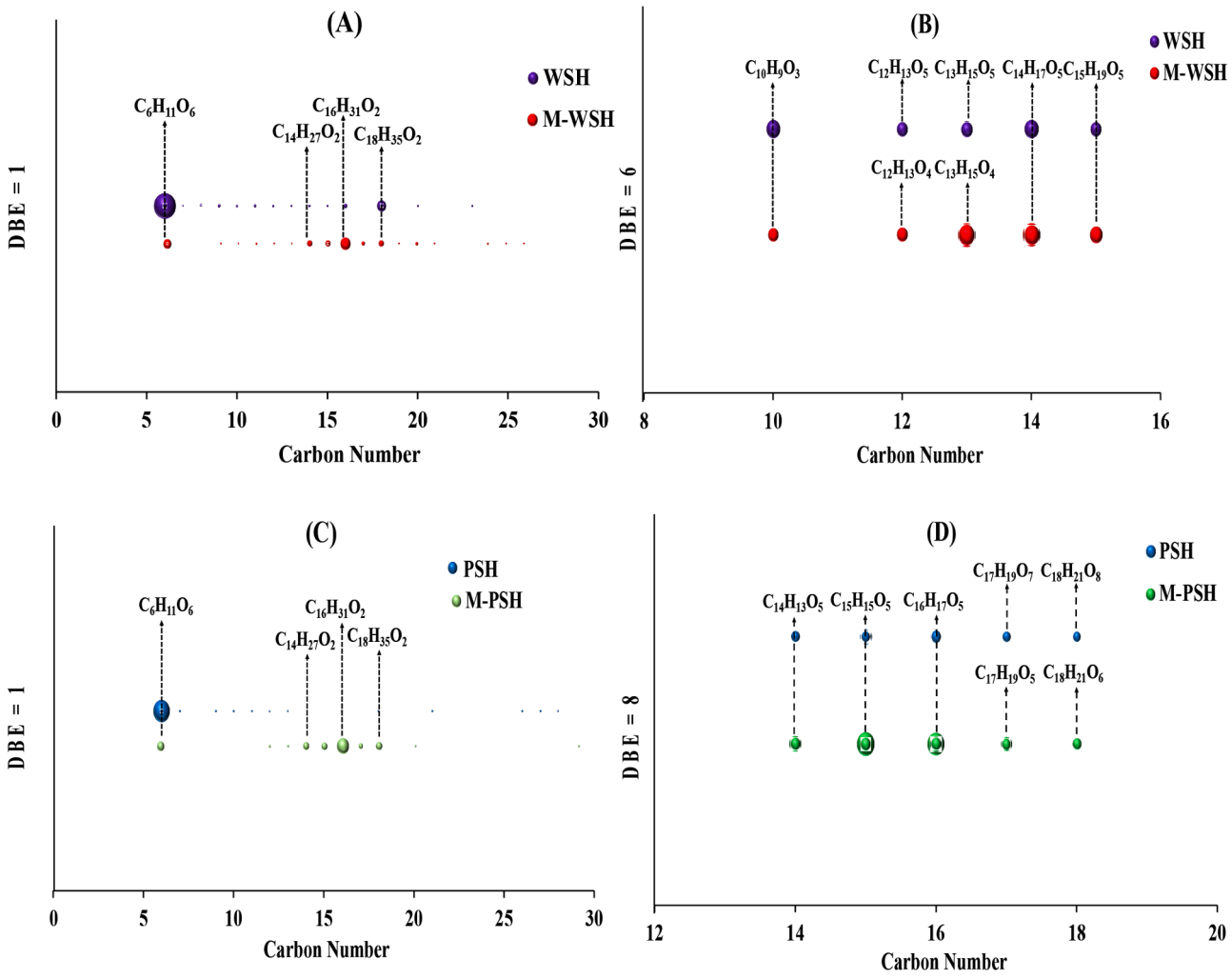

Fig. 5. The carbon number of most abundant compounds versus DBE with the value of 1 in the DOM of WSH and M-WSH (A) and PSH and M-PSH (B); the carbon number of most abundant compounds versus DBE with the value of 6 in the DOM of WSH and M-WSH (C); the carbon number of most abundant compounds versus DBE with the value of 8 in the DOM of PSH and M-PSH (D). The selection of DBE value in (A), (B), (C) and (D) was based on the most abundant molecular in WSH, M-WSH, PSH, M-PSH, respectively. The sphere size represents the relative abundance of one type of molecular formula.

with monocyclic aromatic were dominant molecules in the DOM of microbial-aged hydrochars. With the increased abundances of long-chain carboxylic acids, the DOM of microbial-aged hydrochars became more hydrophobic.

The distribution of O_x species (organic compounds with x oxygen atoms) in different hydrochars-based DOM showed that microbial-aging promoted the shift of compounds containing relatively higher O number (>10O class) to those with lower O number (<10O class) in hydrochars-based DOM. In the DOM of M-WSH and M-PSH, abundance of compounds containing O_1–O_4 increased by 43.1% and 97.6%, those containing O_5–O_9 increased by 12.1% and 26.5%, but those in the class greater than O_9 decreased by 1.57- and 2.11-fold. With decreased abundance of molecules containing high O/C compounds (Fig. 2), we assumed that the increase in the class of compounds containing <10O class was not ascribed to the conversion from hydrocarbon species. These results implied that highly oxygenated compounds were degraded into lower-order oxygenated compounds in the hydrochars-based DOM by microbial activity, such as dehydration, decarboxylation, and reduction of carboxylic acid. Additionally, more oxygenated compounds (e.g., phenolics, alcohols, aldehydes, and carboxylic acid intermediates) with <10O class were produced in the DOM after microbial-aging. Upon application to the soil as amendment, these compounds from M-WSH- and M-PSH-based DOM were more readily released into the soil and were susceptible to the microbial consortia because of higher hydrophobicity (Rombolà et al., 2015; Oleszczuk and Kołtowski, 2018; Quan et al., 2020).

3.4. Microbial-aging mitigated the abundances of phenolic acids, phenols and PAH of hydrochar-based DOM

Table 1 shows the results of quantitative analysis of phenolic acids, phenols, and PAH compounds in hydrochars-based DOM. Microbial-aging resulted in a marked decrease in total phenolic acids; the concentration of total phenolic acids in the DOM of M-WSH and M-PSH was only 26.4% and 62.1% of that in WSH and PSH. Phenolic acids are potent allelochemicals in the soil and has been demonstrated to increase the number of pathogenic microorganisms, such as *Kosakonia sacchari* and *Talaromyuces helices* (Wu et al., 2016), and indirectly cause autotoxicity in monocultured plants (Wu et al., 2017). The reduced phenolic acid content in DOM by microbial-aging is beneficial to the health of soil and plants. Moreover, similar varying trends were also detected in phenols and PAHs. Irrespective of feedstock the total phenols in microbial-aged hydrochars were approximately 1% of that in the pristine hydrochars. The concentration of most phenols was too low to be detected in the DOM of M-WSH or M-PSH. Lignin was an abundant polymer in wheat straw and poplar sawdust, which mainly cracked into

Table 1
The concentration of total phenolic acids, phenols, and PAH in the hydrochars-based DOM.

Chemical compounds		WSH	M-WSH	PSH	M-PSH
Total phenolic acids (mg L^{-1})[a]		20.35	5.38	14.84	9.23
Phenols (mg L^{-1})[b]					
1	Hydroxybenzene	1.05	0.016	0.44	0.0072
2	2-Chlorophenol	0.064	ND[d]	0.017	ND
3	2-Methylphenol	0.20	ND	0.084	0.0029
4	3,4-Methylphenol	0.57	0.0054	0.38	ND
5	2,4-Dimethylphenol	0.13	ND	0.048	ND
6	2,6-Dimethoxyphenyl	0.032	ND	ND	ND
7	4-Ethylphenol	0.051	ND	0.034	ND
∑Phenols		2.09	0.021	1.01	0.010
PAHs (μg L^{-1})[c]					
8	Naphthalene	18.8	1.4	15.2	3.1
9	Acenaphthylene	0.53	ND	0.46	ND
10	Acenaphthene	0.43	ND	0.42	ND
11	Phenanthrene	2.25	0.72	1.94	0.48
12	Chrysene	9.4	0.89	7.5	0.64
13	Fluoranthene	0.16	ND	ND	ND
∑PAHs		31.57	3.01	25.52	4.22

[a] The concentration of total phenolic acids was measured by summing up the concentration of *p*-coumaric, vanillic, *p*-hydroxybenzoic, syringic, caffeic, ferulic, and sinapic acid.

[b] GC–MS was used for phenol compound analyses. In addition to the phenols shown in the table, the concentration of 2-chlorophenol, 2-nitrophenol, 2,4-dichlorophenol, 2,4,6-trichlorophenol, 2,4,5-trichlorophenol, 2,4-dinitrophenol, 4-nitrophenol, 4,6-dinitro-2-methylphenol, 2-methoxylphenol and pentachlorophenol were too low to be detected in any of the hydrochars-based DOM.

[c] PAH: polycyclic aromatic hydrocarbons.GC–MS was used for PAHs analyses. In addition to the PAHs shown in the table, the concentration of fluorene, anthracene, pyrene, benz[a]anthracene, benzo[b]fluoranthene, benzo[k]fluoranthene, benzoapyrene, indenol[1,23-c,d]pyrene, dibenz[a,h]anthracene, and benzo[g,h,i]perylene were too low to detected in any of the hydrochars-based DOM.

[d] ND: not detected.

the phenols during HTC (Xu et al., 2013). Microbial-aging effectively promoted the degradation of phenol compounds and reduced the risk of these contaminants into the environment. Also, the total PAHs in M-WSH and M-PSH were 9.5% and 16.5% of that in WSH and PSH. The reduction of PAHs in hydrochars-based DOM after microbial-aging was consistent with the reduced abundances of condensed aromatics in AI analysis. Studies have reported that the phenols and PAHs from biochars applied to the soil increased the severity of rhizoctonia foliar blight of soybean by downregulating the immunity-associated genes (Copley et al., 2017). PAHs from biochars-based DOM have been shown to alter the process of reproduction in *Folsomia candida* and inhibit root growth in *Lepidium sativum* (Oleszczuk and Kołtowski, 2018). Therefore, because phenolic acids, phenols, and PAHs are potentially toxic to soil microorganisms or crops, the microbial-aging is potentially feasible way to mitigate the toxicity of hydrochars-based DOM.

4. Conclusions

This study demonstrates that microbial-aging changed the molecular composition of hydrochars-based DOM in a positive manner with less aromaticity, higher biodegradability and hydrophobicity, and a lower concentration of phenolic acids, phenols, and PAHs. The comprehensive characterization of hydrochars-based DOM offered an important dataset for future research at molecular level, which can be used to develop environmental-friendly hydrochar materials. In the follow-up studies the dynamic evolution of DOM composition in different microbial-aging stages and fate of microbial-aged hydrochars-based DOM in the soil or water environment need to be investigated.

CRediT authorship contribution statement

QC performed the conceptualization and data curation; DL and HH performed the formal analysis; YF supervised the work; YF and LX acquired the resources and performed the project administration; BW and LH performed the work visualization; QC performed the writing of original draft; LY and BX reviewed and edited the manuscript.

Declaration of Competing Interest

The authors declare that they have no known competing financial interests or personal relationships that could have appeared to influence the work reported in this paper.

Acknowledgement

We appreciate Prof. Jianguang Yu and Ms Yahui Zhao in Jiangsu Academy of Agricultural Science for the analysis of phenolic acids and Dr. Dong Cao in Research Center for Eco-environmental Sciences in Chinese Academy of Sciences for the assistance of ESI-FT-ICR-MS analysis. We also appreciate the funding by National Natural Science of Foundation of China (41877090 and 41807099), open funding of Integrated Farming of Ministry of Agriculture and Rural Affairs (202001), Jiangsu Agricultural Science and Technology Independent Innovation Fund Project (CX(19)1007), USDA NIFA Hatch program (MAS 00549) and NSF (CBET 1739884).

Appendix A. Supplementary data

Supplementary data to this article can be found online at https://doi.org/10.1016/j.biortech.2020.124411.

References

Awasthi, M.K., Wang, Q., Ren, X., Zhao, J., Huang, H., Awasthi, S.K., Lahori, A.H., Li, R., Zhou, L., Zhang, Z., 2016. Role of biochar amendment in mitigation of nitrogen loss and greenhouse gas emission during sewage sludge composting. Bioresour. Technol. 219, 270–280. https://doi.org/10.1016/j.biortech.2016.07.128.

Blum, U., Wentworth, T.R., Klein, K., Worsham, A.D., King, L.D., Gerig, T.M., Lyu, S.-W., 1991. Phenolic acid content of soils from wheat-no till, wheat-conventional till, and fallow-conventional till soybean cropping systems. J. Chem. Ecol. 17 (6), 1045–1068. https://doi.org/10.1007/BF01402933.

Chu, Q., Sha, Z., Osaki, M., Watanabe, T., 2017. Contrasting effects of cattle manure applications and root-induced changes on heavy metal dynamics in the rhizosphere of soybean in an acidic haplic fluvisol: a chronological pot experiment. J. Agric. Food Chem. 65 (15), 3085–3095. https://doi.org/10.1021/acs.jafc.6b05813.s001.

Chu, Q., Xu, S., Xue, L., Liu, Y., Feng, Y., Yu, S., Yang, L., Xing, B., 2020a. Bentonite hydrochar composites mitigate ammonia volatilization from paddy soil and improve nitrogen use efficiency. Sci. Total Environ. 718, 137301. https://doi.org/10.1016/j.scitotenv.2020.137301.

Chu, Q., Xue, L., Cheng, Y., Liu, Y., Feng, Y., Yu, S., Meng, L., Pan, G., Hou, P., Duan, J., Yang, L., 2020b. Microalgae-derived hydrochar application on rice paddy soil: Higher rice yield but increased gaseous nitrogen loss. Sci. Total Environ. 717, 137127. https://doi.org/10.1016/j.scitotenv.2020.137127.

Chu, Q., Xue, L., Singh, B.P., Yu, S., Müller, K., Wang, H., Feng, Y., Pan, G., Zheng, X., Yang, L., 2020c. Sewage sludge-derived hydrochar that inhibits ammonia volatilization, improves soil nitrogen retention and rice nitrogen utilization. Chemosphere 245, 125558. https://doi.org/10.1016/j.chemosphere.2019.125558.

Cimò, G., Kucerik, J., Berns, A.E., Schaumann, G.E., Alonzo, G., Conte, P., 2014. Effect of heating time and temperature on the chemical characteristics of biochar from poultry manure. J. Agric. Food Chem. 62 (8), 1912–1918. https://doi.org/10.1021/jf405549z.

Copley, T., Bayen, S., Jabaji, S., 2017. Biochar amendment modifies expression of soybean and Rhizoctonia solani genes leading to increased severity of rhizoctonia foliar blight. Front. Plant Sci. 8 https://doi.org/10.3389/fpls.2017.00221.

Deaver, J.A., Diviesti, K.I., Soni, M.N., Campbell, B.J., Finneran, K.T., Popat, S.C., 2020. Palmitic acid accumulation limits methane production in anaerobic co-digestion of fats, oils and grease with municipal wastewater sludge. Chem. Eng. J. 396, 125235. https://doi.org/10.1016/j.cej.2020.125235.

dos Santos, J.V., Fregolente, L.G., Moreira, A.B., Ferreira, O.P., Mounier, S., Viguier, B., Hajjoul, H., Bisinoti, M.C., 2020. Humic-like acids from hydrochars: study of the metal complexation properties compared with humic acids from anthropogenic soils using PARAFAC and time-resolved fluorescence. Sci. Total Environ. 722, 137815. https://doi.org/10.1016/j.scitotenv.2020.137815.

Garlapalli, R.K., Wirth, B., Reza, M.T., 2016. Pyrolysis of hydrochar from digestate: effect of hydrothermal carbonization and pyrolysis temperatures on pyrochar formation. Bioresour. Technol. 220, 168–174. https://doi.org/10.1016/j.biortech.2016.08.071.

Ge, S., Usack, J.G., Spirito, C.M., Angenent, L.T., 2015. Long-term n-caproic acid production from yeast-fermentation beer in an anaerobic bioreactor with continuous product extraction. Environ. Sci. Technol. 49 (13), 8012–8021. https://doi.org/10.1021/acs.est.5b00238.

Haeldermans, T., Campion, L., Kuppens, T., Vanreppelen, K., Cuypers, A., Schreurs, S., 2020. A comparative techno-economic assessment of biochar production from different residue streams using conventional and microwave pyrolysis. Bioresour. Technol. 318, 124083. https://doi.org/10.1016/j.biortech.2020.124083.

Hall, S.J., Ye, C., Weintraub, S.R., Hockaday, W.C., 2020. Molecular trade-offs in soil organic carbon composition at continental scale. Nat. Geosci. https://doi.org/10.1038/s41561-020-0634-x.

Hao, S., Zhu, X., Liu, Y., Qian, F., Fang, Z., Shi, Q., Zhang, S., Chen, J., Ren, Z.J., 2018. Production temperature effects on the structure of hydrochar-derived dissolved organic matter and associated toxicity. Environ. Sci. Technol. 52 (13), 7486–7495. https://doi.org/10.1021/acs.est.7b04983.s004.

Harvey, O.R., Kuo, L.-J., Zimmerman, A.R., Louchouarn, P., Amonette, J.E., Herbert, B. E., 2012. An index-based approach to assessing recalcitrance and soil carbon sequestration potential of engineered black carbons (biochars). Environ. Sci. Technol. 46 (3), 1415–1421. https://doi.org/10.1021/es2040398.

Hua, Y., Zheng, X., Xue, L., Han, L., He, S., Mishra, T., Feng, Y., Yang, L., Xing, B., 2020. Microbial aging of hydrochar as a way to increase cadmium ion adsorption capacity: Process and mechanism. Bioresour. Technol. 300, 122708. https://doi.org/10.1016/j.biortech.2019.122708.

Huang, X., Shen, C., Liu, J., Lu, L., 2015. Improved volatile fatty acid production during waste activated sludge anaerobic fermentation by different bio-surfactants. Chem. Eng. J. 264, 280–290. https://doi.org/10.1016/j.cej.2014.11.078.

Koch, B.P., Dittmar, T., 2006. From mass to structure: an aromaticity index for high-resolution mass data of natural organic matter. Rapid Commun. Mass Spectrom. 20 (5), 926–932. https://doi.org/10.1002/rcm.2386.

Liu, Y., Dai, Q., Jin, X., Dong, X., Peng, J., Wu, M., Liang, N.i., Pan, B.o., Xing, B., 2018. Negative impacts of biochars on urease activity: high ph, heavy metals, polycyclic aromatic hydrocarbons, or free radicals? Environ. Sci. Technol. 52 (21), 12740–12747. https://doi.org/10.1021/acs.est.8b00672.s001.

Lopez-Capel, E., Sohi, S.P., Gaunt, J.L., Manning, D.A.C., 2005. Use of thermogravimetry-differential scanning calorimetry to characterize modelable soil organic matter fractions. Soil Sci. Soc. Am. J. https://doi.org/10.2136/sssaj2005.0930.

Oleszczuk, P., Kołtowski, M., 2018. Changes of total and freely dissolved polycyclic aromatic hydrocarbons and toxicity of biochars treated with various aging processes. Environ. Pollut. 237, 65–73. https://doi.org/10.1016/j.envpol.2018.01.073.

Ponnusamy, V.K., Nagappan, S., Bhosale, R.R., Lay, C.-H., Duc Nguyen, D., Pugazhendhi, A., Chang, S.W., Kumar, G., 2020. Review on sustainable production of biochar through hydrothermal liquefaction: physico-chemical properties and applications. Bioresour. Technol. 310, 123414. https://doi.org/10.1016/j.biortech.2020.123414.

Quan, G., Fan, Q., Zimmerman, A.R., Sun, J., Cui, L., Wang, H., Gao, B., Yan, J., 2020. Effects of laboratory biotic aging on the characteristics of biochar and its water-soluble organic products. J. Hazard. Mater. 382, 121071. https://doi.org/10.1016/j.jhazmat.2019.121071.

Riedel, T., Biester, H., Dittmar, T., 2012. Molecular fractionation of dissolved organic matter with metal salts. Environ. Sci. Technol. 46 (8), 4419–4426. https://doi.org/10.1021/es203901u.

Rodríguez-Méndez, R., Le Bihan, Y., Béline, F., Lessard, P., 2017. Long chain fatty acids (LCFA) evolution for inhibition forecasting during anaerobic treatment of lipid-rich wastes: case of milk-fed veal slaughterhouse waste. Waste Manage. 67, 51–58. https://doi.org/10.1016/j.wasman.2017.05.028.

Rombolà, A.G., Marisi, G., Torri, C., Fabbri, D., Buscaroli, A., Ghidotti, M., Hornung, A., 2015. Relationships between chemical characteristics and phytotoxicity of biochar from poultry litter pyrolysis. J. Agric. Food Chem. 63 (30), 6660–6667. https://doi.org/10.1021/acs.jafc.5b01540.

Sha, Z., Chen, Z., Feng, Y., Xue, L., Yang, L., Cao, L., Chu, Q., 2020. Minerals loaded with oxygen nanobubbles mitigate arsenic translocation from paddy soils to rice. J. Hazard. Mater. 398, 122818. https://doi.org/10.1016/j.jhazmat.2020.122818.

Smith, C.R., Hatcher, P.G., Kumar, S., Lee, J.W., 2016. Investigation into the sources of biochar water-soluble organic compounds and their potential toxicity on aquatic microorganisms. ACS Sustainable Chem. Eng. 4 (5), 2550–2558. https://doi.org/10.1021/acssuschemeng.5b01687.s001.

Song, C., Shan, S., Yang, C., Zhang, C., Zhou, X., Ma, Q., Yrjälä, K., Zheng, H., Cao, Y., 2020. The comparison of dissolved organic matter in hydrochars and biochars from pig manure. Sci. Total Environ. 720, 1–8. https://doi.org/10.1016/j.scitotenv.2020.137423.

Stenson, A.C., 2008. Reversed-phase chromatography fractionation tailored to mass spectral characterization of humic substances. Environ. Sci. Technol. 42 (6), 2060–2065. https://doi.org/10.1021/es7022412.

Stenson, A.C., Landing, W.M., Marshall, A.G., Cooper, W.T., 2002. Ionization and fragmentation of humic substances in electrospray ionization fourier transform-ion cyclotron resonance mass spectrometry. Anal. Chem. 74 (17), 4397–4409. https://doi.org/10.1021/ac020019f.

Stenson, A.C., Marshall, A.G., Cooper, W.T., 2003. Exact masses and chemical formulas of individual Suwannee river fulvic acids from ultrahigh resolution electrospray ionization Fourier transform ion cyclotron resonance mass spectra. Anal. Chem. 75 (6), 1275–1284. https://doi.org/10.1021/ac026106p.

Sun, K., Han, L., Yang, Y., Xia, X., Yang, Z., Wu, F., Li, F., Feng, Y., Xing, B., 2020. Application of hydrochar altered soil microbial community composition and the molecular structure of native soil organic carbon in a paddy soil. Environ. Sci. Technol. 54 (5), 2715–2725. https://doi.org/10.1021/acs.est.9b05864.s001.

Sztancs, G., Juhasz, L., Nagy, B.J., Nemeth, A., Selim, A., Andre, A., Toth, A.J., Mizsey, P., Fozer, D., 2020. Co-hydrothermal gasification of Chlorella vulgaris and hydrochar: the effects of waste-to-solid biofuel production and blending concentration on biogas generation. Bioresour. Technol. 302, 122793. https://doi.org/10.1016/j.biortech.2020.122793.

Wang, H., Lu, L.u., Chen, H., McKenna, A.M., Lu, J., Jin, S., Zuo, Y.i., Rosario-Ortiz, F.L., Ren, Z.J., 2020a. Molecular transformation of crude oil contaminated soil after bioelectrochemical degradation revealed by FT-ICR mass spectrometry. Environ. Sci. Technol. 54 (4), 2500–2509. https://doi.org/10.1021/acs.est.9b06164.s001.

Wang, L., Miao, X., Ali, J., Lyu, T., Pan, G., 2018. Quantification of oxygen nanobubbles in particulate matters and potential applications in remediation of anaerobic environment. ACS Omega 3 (9), 10624–10630. https://doi.org/10.1021/acsomega.8b00784.s001.

Wang, T., Si, B., Gong, Z., Zhai, Y., Cao, M., Peng, C., 2020b. Co-hydrothermal carbonization of food waste-woody sawdust blend: Interaction effects on the hydrochar properties and nutrients characteristics. Bioresour. Technol. 316, 123900. https://doi.org/10.1016/j.biortech.2020.123900.

Wiedner, K., Naisse, C., Rumpel, C., Pozzi, A., Wieczorek, P., Glaser, B., 2013. Chemical modification of biomass residues during hydrothermal carbonization – what makes the difference, temperature or feedstock? Org. Geochem. 54, 91–100. https://doi.org/10.1016/j.orggeochem.2012.10.006.

Wu, H., Wu, L., Wang, J., Zhu, Q., Lin, S., Xu, J., Zheng, C., Chen, J., Qin, X., Fang, C., Zhang, Z., Azeem, S., Lin, W., 2016. Mixed phenolic acids mediated proliferation of pathogens Talaromyces helicus and Kosakonia sacchari in continuously monocultured radix pseudostellariae rhizosphere soil. Front. Microbiol. 7 https://doi.org/10.3389/fmicb.2016.00335.

Wu, H., Xu, J., Wang, J., Qin, X., Wu, L., Li, Z., Lin, S., Lin, Weiwei, Zhu, Q., Khan, M.U., Lin, Wenxiong, 2017. Insights into the mechanism of proliferation on the special microbes mediated by phenolic acids in the radix pseudostellariae rhizosphere under continuous monoculture regimes. Front. Plant Sci. doi: 10.3389/fpls.2017.00659.

Xu, Q., Qian, Q., Quek, A., Ai, N., Zeng, G., Wang, J., 2013. Hydrothermal carbonization of macroalgae and the effects of experimental parameters on the properties of hydrochars. ACS Sustainable Chem. Eng. 1 (9), 1092–1101. https://doi.org/10.1021/sc400118f.

Yang, E., Meng, J., Hu, H., Cheng, D., Zhu, C., Chen, W., 2019. Effects of organic molecules from biochar-extracted liquor on the growth of rice seedlings. Ecotoxicol. Environ. Saf. 170, 338–345. https://doi.org/10.1016/j.ecoenv.2018.11.108.

Yu, S., Feng, Y., Xue, L., Sun, H., Han, L., Yang, L., Sun, Q., Chu, Q., 2019a. Biowaste to treasure: application of microbial-aged hydrochar in rice paddy could improve nitrogen use efficiency and rice grain free amino acids. J. Cleaner Prod. 240, 118180. https://doi.org/10.1016/j.jclepro.2019.118180.

Yu, Z., Liu, X., Chen, C., Liao, H., Chen, Z., Zhou, S., 2019b. Molecular insights into the transformation of dissolved organic matter during hyperthermophilic composting using ESI FT-ICR MS. Bioresour. Technol. 292, 122007. https://doi.org/10.1016/j.biortech.2019.122007.

Yuan, R., Shen, Y., Zhu, N., Yin, C., Yuan, H., Dai, X., 2019. Pretreatment-promoted sludge fermentation liquor improves biological nitrogen removal: molecular insight into the role of dissolved organic matter. Bioresour. Technol. 293, 122082. https://doi.org/10.1016/j.biortech.2019.122082.

Zhou, X.-F., 2014. Conversion of kraft lignin under hydrothermal conditions. Bioresour. Technol. 170, 583–586. https://doi.org/10.1016/j.biortech.2014.08.076.

Zhu, N., Zhang, J., Tang, J., Zhu, Y., Wu, Y., 2018. Arsenic removal by periphytic biofilm and its application combined with biochar. Bioresour. Technol. 248, 49–55. https://doi.org/10.1016/j.biortech.2017.07.026.